

Optimization of Methyl Orange Dye Photodegradation Using TiO₂/Porous Ceramics with Response Surface Methodology

Diana Eka Pratiwi¹, Suriati Eka Putri^{1*}, Sumiati Side¹, Rizal Irfandi¹, Muhammad Taufiq¹, Abd Rahman²

¹Chemistry Department, Universitas Negeri Makassar, Indonesia

²Chemistry Department, King Fahd University of Petroleum & Minerals, Dhahran, Saudi Arabia

*E-mail: ekaputri_chem@unm.ac.id

DOI: <https://doi.org/10.26874/jkk.v8i1.917>

Received: 14 May 2025, Revised: 17 June 2025, Accepted: 17 June 2025, Online: 20 June 2025

Abstract

Environmental pollution from dye waste is one of the environmental problems that is of concern today. One method that is effective, reliable, and does not require a large cost is photodegradation. In this study, a TiO₂/porous ceramic (TiO₂/PC) photocatalyst was used which was synthesized by the sol-gel coating method. The resulting photocatalyst was then characterized using XRF, XRD, SEM, and SAA which were then applied to the photodegradation process of methyl orange (MO) dyestuffs. Optimization of photodegradation conditions of MO dyes using porous TiO₂/PC catalysts was carried out using the Response Surface Methodology (RSM) method by Central Composite Design (CCD). The characterization results showed that the TiO₂ phase was in the rutile phase with a level of 10.35%. The resulting photocatalyst has pores on the surface covered by TiO₂ with a shrinking pore volume after impregnation from 0.076637 cm³/g to 0.064943 cm³/g with an average pore diameter from 4.51187 nm to 4.49999 nm. The optimal condition of degradation of MO dye occurred at pH 6, an initial concentration of 25 mg/L for 120 minutes, with a percentage of degradation of 89.54% and can be used up to four cycles. Thus, TiO₂/PC photocatalysts have the potential to be used in the process of processing MO dye waste.

Keywords: Photocatalyst, Photodegradation, Porous ceramic

1 Introduction

The availability of safe drinking water and clean water sanitation are the main resources to ensure human well-being. However, the rapid development of industry has caused water pollution in the environment. One of the largest wastes that is directly discharged into the environment is dye [1,2]. Dye waste that is discharged into the environment without further processing is toxic with potential carcinogenic and genotoxic effects [3]. One of the dyes that is widely used on an industrial scale and cannot be naturally decomposed is methyl orange (MO) dye [4]. This is because MO dye contains a benzene group so it has carcinogenic properties and takes a long time to degrade [5].

Therefore, a method to degrade MO dyes is required. Several methods that have been used in wastewater treatment processes are adsorption, coagulation, precipitation, photodegradation, ion exchange, and electrochemistry [6]. Among these

methods, photodegradation is a method that is widely used because it uses photocatalysts that can be mass-produced, are effective, and reliable in processing dye waste [7]. In general, the photocatalysts used are metal oxides, such as ZnO [8], TiO₂ [9], Fe₂O₃ [10], PbO [11], and CuO [12]. Among these photocatalysts, TiO₂ is the most widely studied because it has several advantages, including having a small band gap. This characteristics are able to facilitate the occurrence of photoreduction and photo-oxidation reactions through the process of electron excitation from the valence band and conduction band with the help of UV light [9]. Through this mechanism, •OH and •O₂⁻ radicals are formed which will then degrade the complex dye structure into a simpler structure [7].

Several previous studies reported that the efficiency and effectiveness of TiO₂ catalysts can be improved by using catalyst supports. Several materials that have been used as catalyst supports



for the photodegradation process are zeolite, alumina, silica, and activated carbon [13,14]. However, the catalyst supports are in powder form, a separation stage is still needed after the degradation process. Therefore, in this study we tried to use advanced materials in the form of pellets which are superior and preferred by the industry because they are easy to separate and can be used repeatedly. The use of TiO_2 /porous ceramic catalysts has several advantages, namely easy to reuse because they are easy to separate, have high resistance, and the TiO_2 leaching process on the catalyst surface can be avoided [15,16]. The advanced pellet-shaped material used in this study is porous ceramics. The use of porous ceramics in catalytic reactions has been studied in recent years, including in the H_2 synthesis process [17], styrene synthesis [18], biodiesel production [19] and phenol degradation [10]. The porous ceramics used in this study are prototypes that have been produced in previous studies that were synthesized from natural clay and cassava starch by gelcasting [20].

In the laboratory-scale photodegradation process, it is carried out in aqueous solutions, so that optimum conditions are needed for industrial application. One way to determine optimum conditions is to use Response Surface Methodology (RSM). Several experimental plans such as 3k factorial, Doehlert, Box-Behnken, and Central Composite Design (CCD) have been used for this process [21]. Among these models, CCD is the most commonly used method to control optimal conditions and the influence of each independent variable, which is considered an advantage of this statistical method [22]. Based on literature studies that have been carried out, several independent variables that affect the photodegradation process are solution pH, irradiation time, and catalyst dose.

Several previous studies have used CCD-based RSM to optimize the efficiency of photodegradation of various types of dyes from aqueous solutions [23,12]. However, previous studies have never used TiO_2 photocatalyst supported by porous ceramics in the form of pellets. Thus, its application in the process of optimizing the photodegradation of MO dyes using TiO_2 /porous ceramics is a new innovation that will be discussed in this paper. To the best of our knowledge, this is the first report to combine pelletized TiO_2 /porous ceramic photocatalysts with RSM optimization for the photodegradation of methyl orange dye. This study offers a scalable,

reusable, and efficient system for industrial wastewater treatment applications.

2 Method

The research consists of impregnation of TiO_2 into porous ceramic, characterization of TiO_2 /porous ceramic, and optimization of photodegradation conditions of methyl orange dye. The porous ceramics used were prototypes that had been produced in our previous research with a cassava starch percentage of 6% [15,20,24]. The impregnation method was carried out using the sol gel coating method. The metal oxide precursor used was titanium nitrate salt ($\text{Ti}(\text{NO}_3)_4$) dissolved in 50 mL of distilled water, then 5 mL of ethylene glycol was added and stirred for 1 hour. Furthermore, one porous ceramic pellet was added to the solution. The impregnation process was carried out under vacuum conditions as shown in **Fig. 1**. The impregnated ceramics were then calcined at a temperature of 400°C . The resulting catalyst was labeled TiO_2/PC .



Figure 1 The illustration of impregnation process at vacuum condition

The resulting TiO_2/PC catalyst was then analyzed for metal oxide content using X-Ray Fluorescence (XRF, Shimadzu EMX-720/800 HS), crystal phase analysis using X-Ray Diffractometer (XRD, Shimadzu 7000), surface morphology analysis using Scanning Electron Microscope (SEM, JEOL JCM 6063LA), and Surface Area Analyzer (SAA, Quantachrome Nova 4200e).

Optimization of photodegradation conditions was carried out using Design Expert® 13.0.5.0 software with the RSM method through CCD design. In this study, three independent variables (input factors) were used which are factors that affect the photodegradation process of MO dyes and have been studied by several previous studies, namely pH, irradiation time, and catalyst dose. The dependent variable is the percentage of

degradation obtained from the calculation of the difference in dye concentration before and after the degradation process. The dye solution was loaded into the photodegradation reactor as shown in **Fig. 2**. It was stirred at 100 rpm during the irradiation process using UV lamp (Philips TUV 15W/G15 T8 - λ 280 nm). Separation was carried out using centrifugation at a speed of 7000 rpm for 15 min, then the absorbance of the remaining dye was measured using a Shimadzu UV-Vis Spectrophotometer.

The recycling test was carried out by separating the pelletized TiO₂/PC from the dye solution, then the catalyst was washed in methanol and stirred for 1 hour, and dried at 100 °C for 12 hours.

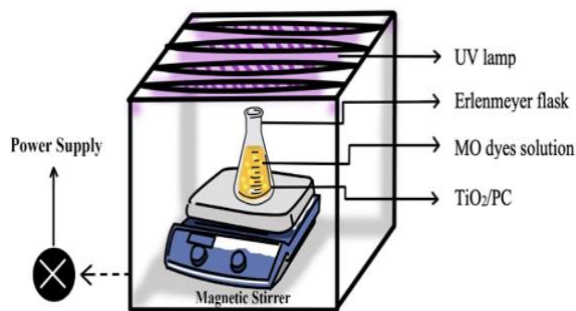
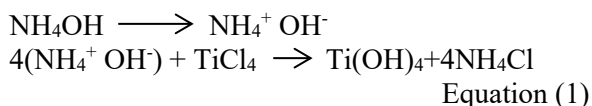


Figure 2 The illustration of reactor for degradation MO using TiO₂/PC

3 Result and Discussion

The photocatalyst synthesis method used in this study is the wet impregnation method of Ti(NO₃)₄ precursors into porous ceramics in a gel coating. The sol-gel coating method is a method that aims to grow a thin layer on the surface of porous material evenly. The sol-gel coating method begins by mixing TiO₂ with HCl which will become a TiCl₄ solution, then adding a solution resulting from mixing NH₄OH solution and (NH₄)₂SO₄ solution as a source of OH ions and the result of this mixing will form a Ti(OH)₄ solution which will later fill the pores and coat the ceramic surface. The reaction that occurs is shown in **Eq. 1**.



The mixture is stirred using a magnetic stirrer for 6 hours at a temperature of 85°C which aims to accelerate the process of forming Ti(OH)₄. The stirring and heating process aims to make the solution in the sol-gel phase which will then form a thin layer on the ceramic surface. Then it is

dipped in the solution while still stirring for 5 minutes then calcination is carried out at a temperature of 600 °C for 3 hours to oxidize Ti(OH)₄ into TiO₂.

3.1 Characterization of TiO₂/PC

Characterization using XRF was used to determine the levels of metal oxides contained in porous ceramics both before TiO₂ impregnation and after TiO₂ impregnation. The results of XRF analysis are shown in **Table 1**, proving an increase in TiO₂ levels from 0.92% to 10.35%.

Table 1 XRF Instrument Analysis Results of Porous Ceramic Metal Oxide Content Before and After Impregnation

Metal Oxides	Content (%)	
	PC	TiO ₂ /PC
SiO ₂	78.08	60.31
Fe ₂ O ₃	7.65	10.33
Al ₂ O ₃	4.84	-
K ₂ O	3.82	2.99
ZnO	2.11	0.023
CaO	1.38	11.16
TiO ₂	0.92	10.35

The next analysis uses XRD which aims to study the structure of TiO₂ crystals found in porous ceramics. Based on the XRD diffractogram in **Fig. 3** shows that porous ceramics after being impregnated with TiO₂ have a peak intensity value of 2θ 26.7°. When compared with the standard TiO₂ rutile data base (JCPDS Card Number 75-1537) with a peak intensity value of 2θ 27.34° and the standard TiO₂ anatase data base (JCPDS Number 21-1272) with a peak intensity value of 2θ 25.23°, it can be concluded that the result of this study is that the TiO₂ crystal phase that has been successfully impregnated is the rutile and anatase phase.

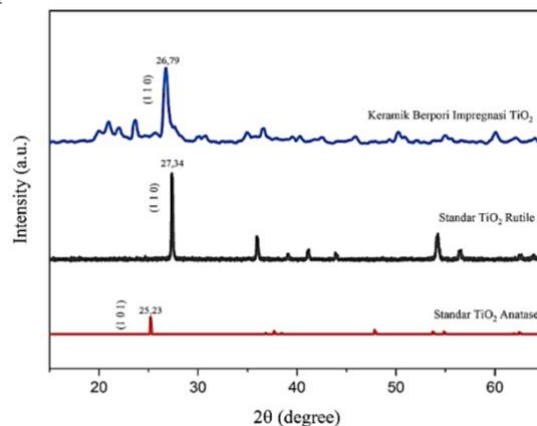


Figure 3 The diffractogram of PC and TiO₂/PC



Morphological characterization of porous ceramics was carried out using the Scanning Electron Microscopy (SEM) instrument, shown in Fig. 4. The morphology of the PC indicates the presence of open pores and closed pores scattered on the surface of the PC with heterogeneous

shapes. After TiO₂ impregnation, it shows that the morphology of the ceramic has changed the shape of the pores from a large size to a smaller size, which indicates that the ceramic pores are covered by a TiO₂ catalyst [10].

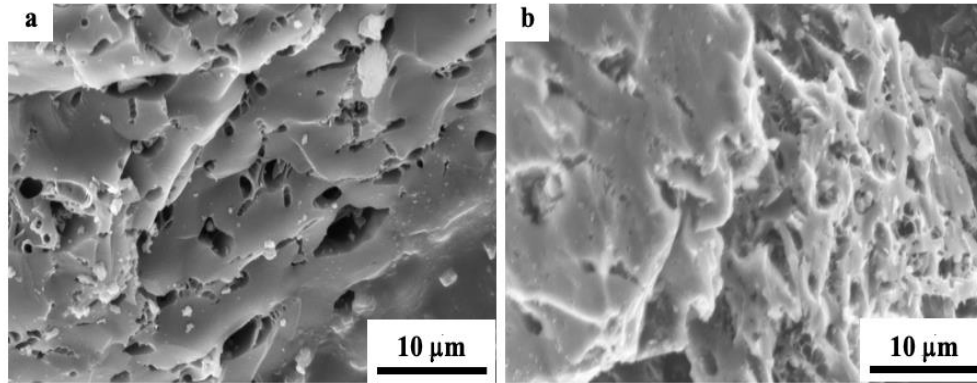


Figure 4 Morphology of (a) PC and (b) TiO₂/PC using SEM with 2000x magnification

The next analysis is the characterization of microstructures in the form of pore characterization of PC and TiO₂/PC. The results of pore characterization were carried out based on N₂ gas adsorption, surface area and pore volume were carried out using the BET method and the average pore diameter was used using the BJH method, shown in Fig. 5 with the results of interpretation in Table 2. Based on the analysis, TiO₂ was obtained

which falls into the category of mesopore with a diameter between 2-50 nm. Based on the adsorption-desorption curve, the characteristics of TiO₂ are close to type IV isotherms and H1 type hysteresis loops based on the IUPAC classification, the material exhibits characteristics of mesoporous structures with an indication of cylindrical pore shape.

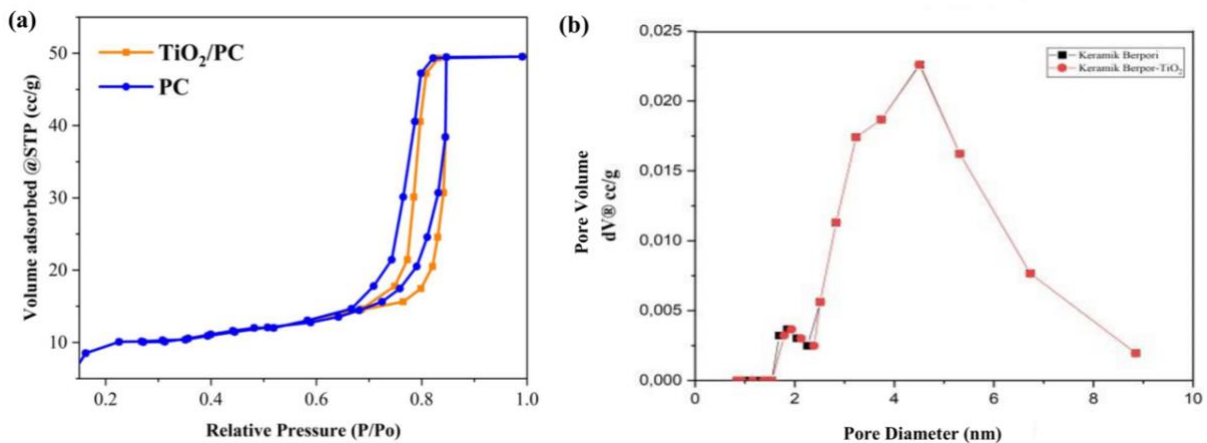


Figure 5 (a) N₂ gas Adsorption-Desorption Curve and (b) BJH Curve

Based on Table 2, there is an increase in the value of the surface area of BET in ceramics that have been impregnated with TiO₂ compared to porous ceramics before impregnation along with the reduction in the value of the pore volume and the average pore diameter. This shows that the smaller the pore diameter size and the volume of the pores, the greater the surface area value. TiO₂ affects the value of surface area when applied as a material [10,15,16]. In addition, the decrease in

pore volume also proves the successful impregnation of TiO₂ into porous ceramics.

Table 2 Analysis Results Surface Area Analyzer

Sample	BET Surface Area (m ² /g)	Pore volume (cm ³ /g)	Average pore diameter (nm)
PC	22.515	0.076637	4.51187
TiO ₂ /PC	22.6091	0.064943	4.49999

Furthermore, to determine the ability of TiO₂/PC in producing radical ions to degrade MO depends on E_g. The E_g in this study was analyzed based on the UV-Vis spectrum, using the Tauc plots' approach to find the relationship between the absorption coefficient (α) and incident photon energy ($\alpha h\nu$) as shown in **Eq. 2**.

$$\alpha h\nu = A (h\nu - E_g)^n \quad (\text{Equation 2})$$

where where α is the absorption coefficient, h is Planck's constant (6.626×10^{-34} J s), ν is the frequency of light, c is the speed of light (3×10^8 m/s), and λ is the wavelength of the spectrum.

The results of the band gap (E_g) calculation analysis based on the Tauc plots' of TiO₂/PC are shown in **Fig. 6**. The calculation results of the Tauc plot approach show that E_g TiO₂/PC is 2,861 eV. The E_g value obtained is lower than the results of previous studies that also used PC as a support for TiO₂ catalysts with a higher calcination temperature [24]. This proves that the TiO₂/PC produced in this study can be used for MO photodegradation.

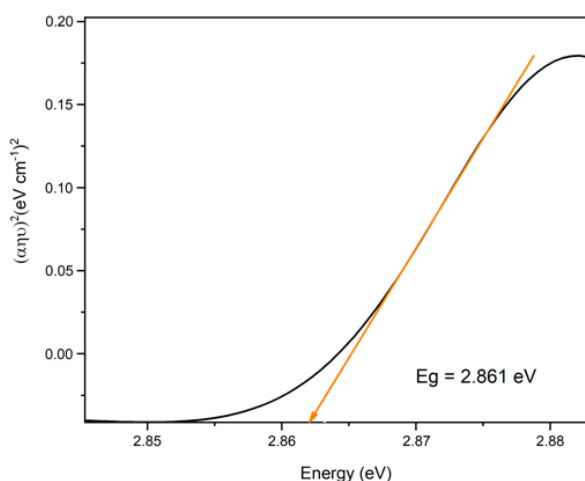


Figure 6 Band gap of TiO₂/PC determined using UV-Vis spectrophotometer by Tauc plots' approach

3.2 Determination of Optimum Conditions for MO Photodegradation Using TiO₂/PC

The determination of the optimum conditions is carried out using the Design Expert software version 13.0.5.0 which also provides statistical data on the data collected. The model of the quadratic polynomial equation was found to match the experimental data and this model was subsequently used to determine the optimal conditions. The results of the ANOVA analysis were used to verify the model equations shown in **Table 3**. The results of the analysis obtained a p-

value of 0.0371 which shows a significant quadratic equation model. Table 3 shows that the pH and irradiation time parameters have a significant influence on the percent degradation shown by p< values of 0.05 (0.0443 and 0.0115). The initial concentration parameter has a p> value of 0.05 (0.1571) which indicates no significant effect on the percentage degradation. However, these three parameters are important free variables in the photodegradation process of MO dyes [21]. It is supported by further analysis using post hoc tests including Least Significant Difference (LSD) and Tukey's Honest Significant Difference (HSD) using a 95% confidence interval on the initial concentration treatment (for example, in runs 4 and 9 with different initial concentrations, the same pH and irradiation time, $2.54 > \text{LSD}$ was obtained).

A polynomial equation where Y is the percent degradation and the equation is predicted from the software after the degradation process on each variation is shown in **Eq. 3**.

$$Y = 84.32 + 7.49A + 11.88B - 1.07C + 3.94AB + 4.18AC - 1.95BC + 5.18A^2 - 15.92B^2 - 6.83C^2 \quad (\text{Equation 3})$$

Table 3 Results of ANOVA analysis using the RSM method

Source	Sum of Squares	df	Mean Square	F-value	p-value	
Model	3043.51	9	338.17	3.86	0.0371	Significant
A-pH	448.80	1	448.80	5.12	0.0443	
B-Initial Concentration	1129.79	1	1129.79	12.89	0.1571	
C-Irradiation Time	9.18	1	9.18	0.1048	0.0115	
AB	62.09	1	62.09	0.7087	0.4321	
AC	70.06	1	70.06	0.7996	0.4057	
BC	15.25	1	15.25	0.1740	0.6911	
A ²	107.28	1	107.28	1.22	0.3109	
B ²	1014.26	1	1014.26	11.58	0.0145	
C ²	186.80	1	186.80	2.13	0.1945	
Residual	525.70	6	87.62			
Lack of Fit	525.69	3	175.23	262.84	< 0.0001	Not Significant
Pure Error	0.0020	3	0.0007			
Cor Total	3569.21	15				

The experimental design obtained based on the range of free variables to the percent response of MO degradation is shown in **Table 4**. The percent degradation of MO ranged from 1.24% to 89.54% in experimental tests at numbers 5 and 13, respectively. The percentage of methyl orange degradation at optimum conditions is higher than our previous research results which only used TiO₂



of 61.78% and only used porous ceramics of 54.56% [24]. It shows that the role of TiO₂ active sites is greater than using only PC. However, the resulting percentage of degradation is lower than previous research using zeolite-supported CdS/TiO₂/Ag₂CO₃ ternary-based composites successfully degraded MO by 91.6% at 10 mg/L for 160 min [25]. Furthermore, previous research showed a higher percentage of degradation also using cellulose nanocrystal templated TiO₂ films with a percentage of MO degradation of 98.0% [26]. This is thought to be due to the small surface

area of PC, but TiO₂/PC shows extraordinary effectiveness because it can be used up to five cycles which have been studied in our previous research [24].

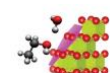
The condition of the photodegradation process with a minimum percent degradation occurs at pH 4.5, initial concentration of 1 mg/L without irradiation time. The photodegradation condition with the largest percentage of degradation occurred at irradiation time 120 minutes, pH 6, and initial concentration of 25 mg/L.

Table 4 Percentage degradation of MO under various reaction conditions

Run	Factor 1 A:pH	Factor 2 B:Initial concentration mg/L	Factor 3 C:Irradiation Time Min	Response Degradation %
1	3	25	5	11.32
2	4.5	13.5	62.5	23.54
3	7	13.5	62.5	34.56
4	3	2	120	25.67
5	4.5	1	0	1.24
6	4.5	13.5	62.5	25.46
7	4.5	13.5	62.5	2.16
8	4.5	13.5	62.5	24.76
9	3	25	120	66.56
10	3	2	5	7.98
11	6	2	5	11.43
12	4.5	13.5	159.2	76.89
13	6	25	120	89.54
14	4.5	13.5	62.5	77.64
15	4.5	13.5	62.5	67.89
16	4.5	32.8	62.5	73.87
17	1.97	13.5	62.5	9.32
18	6	25	5	22.13
19	6	2	120	76.54

The accuracy of the model is checked by the residual analysis plot shown in Figure 7, where a good fit with the formation of linear lines is shown in **Fig. 7(a)**. The compatibility between the experimental results and the predicted results is shown in **Fig. 7(b)**, showing that there is a

suitability of the data along the slope line. Colour indicators ranging from wane blue to red on the chart show the lowest to highest MO degradation percentages [24]. An adequate model is also shown in **Fig. 7(c)** with a random residual pattern where all points are within the desired limit.



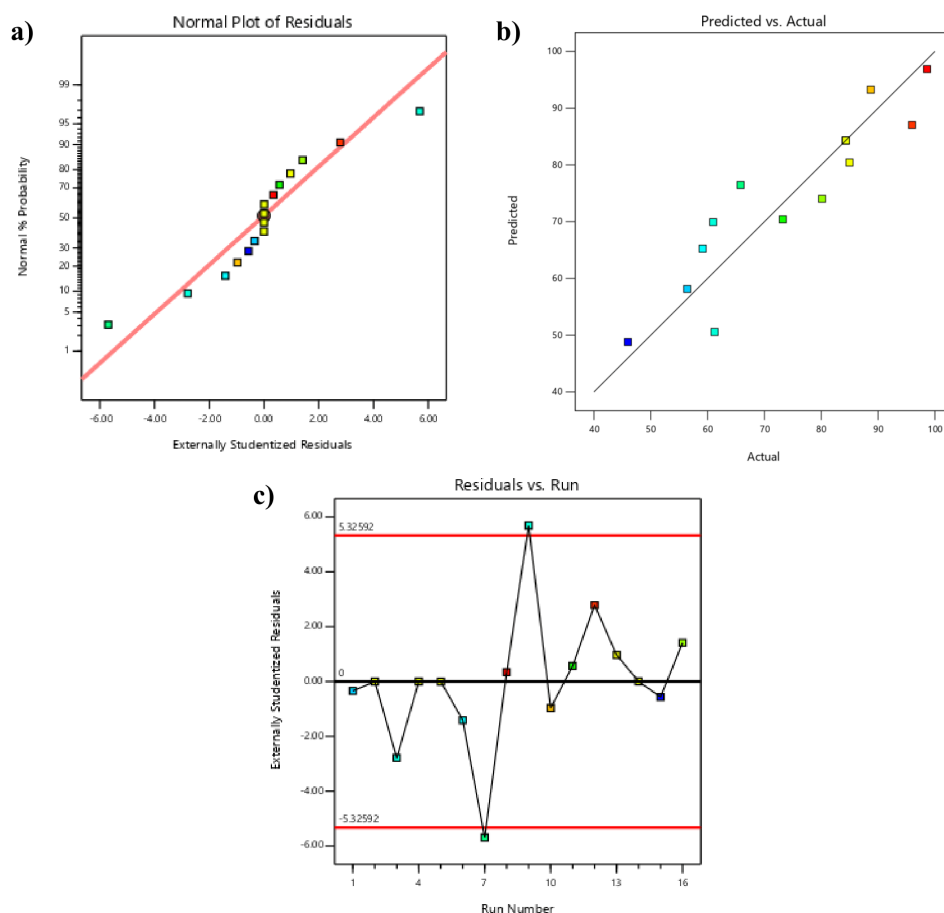


Figure 7 Curve (a) normal distribution of residuals (errors) (b) plot of predicted response variables and experimental results (c) residuals and run orders

Based on the results of the statistical analysis performed and the resulting square model, a three-dimensional diagram of the response procedure and a two-dimensional contour diagram are suitable for illustrating the response. Surface and contour procedure diagrams are used to establish the exact relationship between the response value and the degradation process conditions. In this diagram, the two effective factors of the variable and the other factor are selected as fixed and in the central code (0) to examine the simultaneous changes of the two factors and their influence on each other graphically [25]. The simultaneous interaction of percent degradation by varying initial concentration and pH is shown by the 3D surface response and contour plot in **Fig. 8(a1-a2)**.

The results showed that there was no significant effect of the initial concentration on the performance of the TiO₂/PC catalyst for MO dye degradation, as shown from the p-value in **Table 3** (0.1571, $p > 0.05$). **Fig. 8(b1-b2)** shows the relationship between pH and irradiation time, proving that these two variables affect the percent of MO degradation. This is supported by the data

from the analysis in **Table 3** which has a p value of > 0.05 . The results of the study showed that the higher the irradiation time, the higher the percentage of MO degradation. This is suspected because the longer the interaction between the MO substance and the photocatalyst the more electron hole pairs ($e^- h^+$) the formation of $\bullet OH$ and $\bullet O_2^-$ radicals which will further degrade the complex dye structure to a simpler structure. The results obtained are in line with previous studies that degraded the dye acid orange 7 using copper nanoparticles [7].

The next analysis is the interaction between the initial concentration and irradiation time shown in **Fig. b(c1-c2)**. The results of the study show that the higher the initial concentration of MO, the higher the percentage of MO degradation produced. The results obtained are in line with the results of previous studies that degraded tartrazine yellow dye using TiO₂ [26] Thus, the optimum conditions obtained occurred at pH 6, an initial concentration of 25 mg/L for 120 minutes, with a degradation percentage of 89.54%.



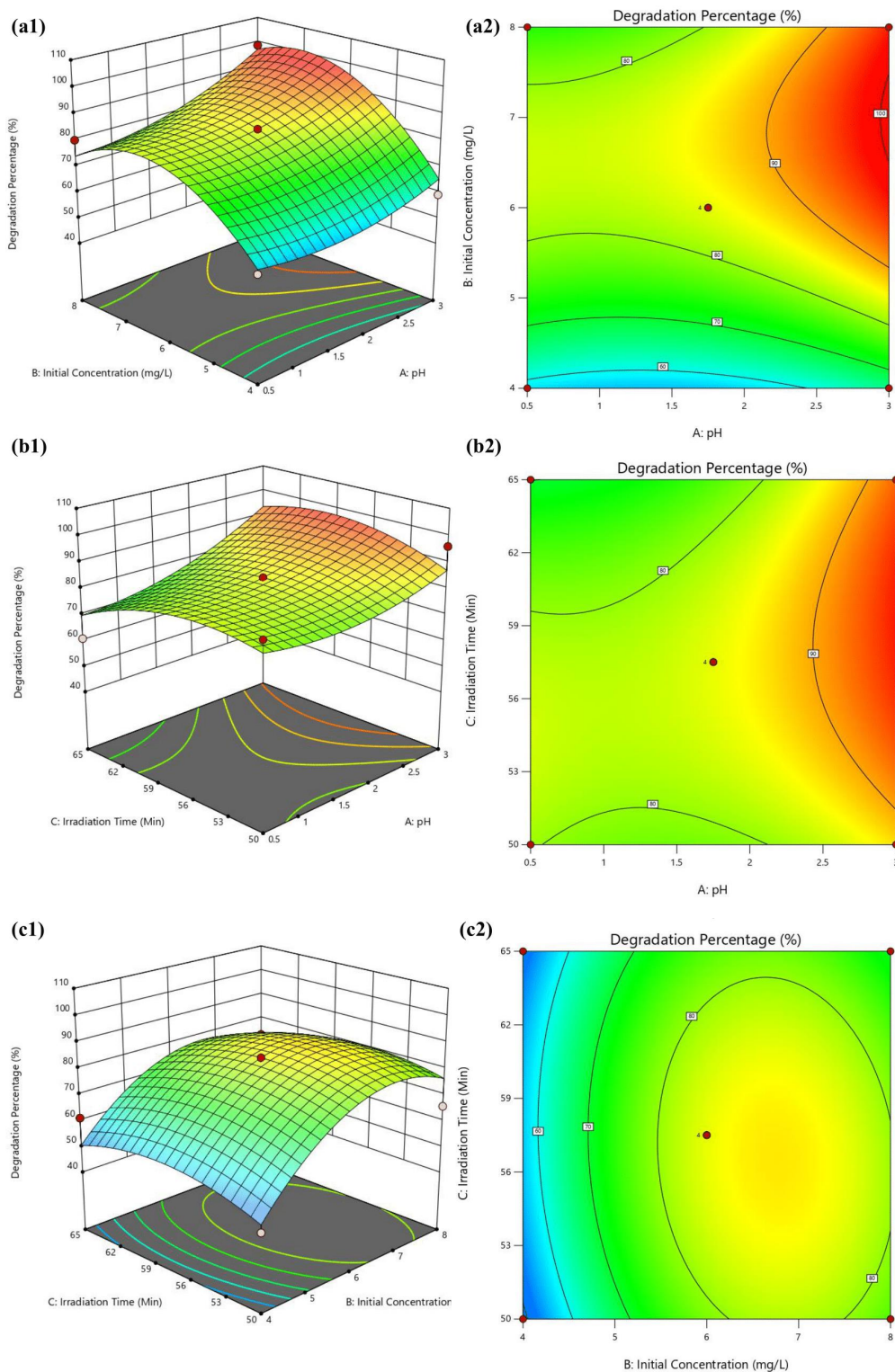


Figure 8 3D surface response interaction and contour plot of the influence of (a) pH and initial concentration, (b) pH and irradiation time, (c) initial concentration and irradiation time

To determine the role of electron-hole scavengers on the photodegradation performance of ZnO/MMT, experiments were carried out through degradation analysis at optimum conditions, namely at pH 6, initial concentration

of 25 mg/L with an irradiation time of 120 minutes. **Fig. 9** shows that the addition of AgNO_3 acts as an electron scavenger which shows the highest photodegradation efficiency of up to $93.78 \pm 0.46\%$ while the performance of

TiO₂/PC+CH₃OH which acts as a hole scavenger produces a degradation percentage of 80.21±0.86%. The results obtained indicate that the addition of AgNO₃ as an electron scavenger can significantly optimize photodegradation activity. With the help of an electron scavenger, the charge recombination rate can be reduced, excited electrons can migrate and produce •OH and •O₂⁻ radicals. As a result, •O₂⁻ reacts with MO dye; thus reducing the concentration of dye in the system [21]. Conversely, the addition of a hole scavenger (CH₃OH) shows lower photocatalytic degradation performance compared to an electron scavenger.

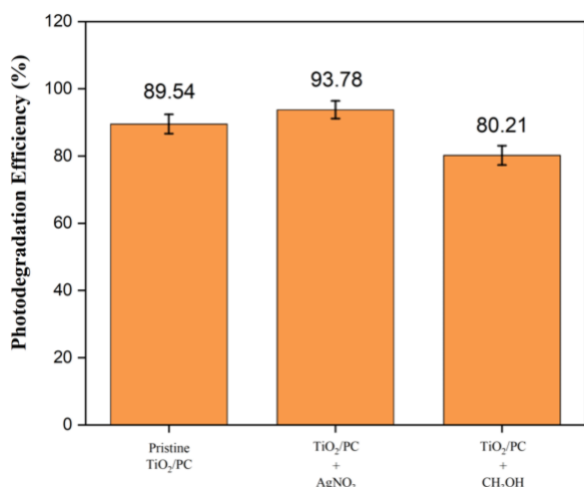


Figure 9 Study of electron-hole scavenger of photodegradation MO using TiO₂/PC

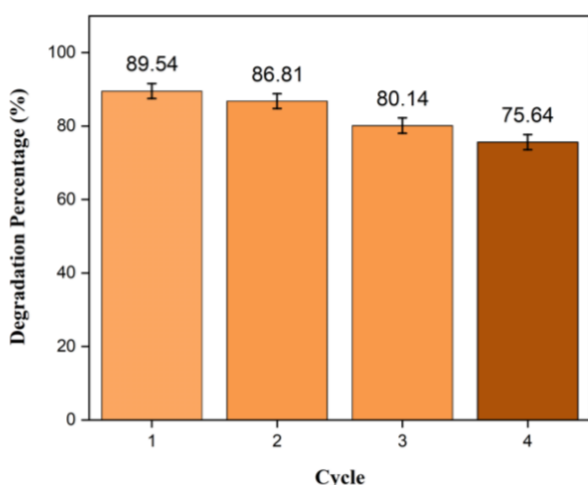


Figure 10. The recyclability test of TiO₂/PC for MO photodegradation

In addition, a recycling test was also carried out by reusing the TiO₂/PC photocatalyst. The results obtained are shown in **Fig. 10**, the resulting photocatalyst can be used up to four cycles. In the second and third cycles, there was a decrease to

86.81±0.02% and 80.14±0.10%, respectively. The percentage of degradation decreased drastically in the fourth cycle with a percentage of degradation of only 75.64±0.08%. The number of cycles that can be used in this study is lower than the use of Fe₂O₃/PC pellet catalysts in the phenol degradation process [10].

This study has several limitations, where the concentration range tested on dye solutions is limited for 1-25 mg/L which is less applicable to the industrial sector that produces higher dye concentrations. Thus, it is very possible to improve the model in RSM either through Central Composite or Box-Behnken design.

4 Conclusion

TiO₂/PC photocatalysts were successfully synthesized using the sol-gel coating method. The resulting photocatalyst showed that the TiO₂ phase was in the rutile phase with a level of 10.35%. The synthesized TiO₂/PC photocatalyst has a surface area of 22.6091 m²/g with a pore volume of 0.064943 cm³/g and an average pore diameter of 4.49999 nm. The optimum condition of degradation of MO dyes obtained from the CCD design occurred at pH 6, an initial concentration of 25 mg/L for 120 minutes, with a degradation percentage of 89.54%. Therefore, therefore, the degradation strategy of MO dyes using TiO₂/PC pellet photocatalyst can provide a new perspective on the textile industry wastewater treatment process. In addition, we conclude that TiO₂/PC is one of the materials with good photocatalytic performance for MO degradation and is promising in applications such as photovoltaic devices, biomedical, and microbiology.

Acknowledgement

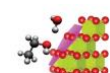
We would like to thank the Institute for Research and Community Service (LP2M) of Universitas Negeri Makassar for the PNBPNBP funding of the Faculty of Mathematics and Natural Sciences which has been provided with contract number: 361/UN36.11/TU/2025.

References

- [1] Choudhary N., Yadav VK., Yadav KK., Almohana AI., Almojil SF., Gnanamoorthy G., ... Jeon BH., 2021, Application of green synthesized MMT/Ag nanocomposite for removal of methylene blue from aqueous solution, *Water*, 13(22), 1-13, 3206. <https://doi.org/10.3390/w13223206>



- [2] Side S., Putri SE., Perdana R., & Rahman A., 2024, Adsorption Kinetics of Cd (II) From Aqueous Solution Using Surfactant Modified Activated Carbon-Sodium Lauryl Sulphate (SMAC-SLS), *Sainsmat: Jurnal Ilmiah Ilmu Pengetahuan Alam*, 13(2), 171-177. <https://doi.org/10.35580/sainsmat132515432024>
- [3] Alikarami S., Soltanizade A., & Rashchi F., 2022, Synthesis of CdS–SnS photocatalyst by chemical co-precipitation for photocatalytic degradation of methylene blue and rhodamine B under irradiation by visible light, *Journal of Physics and Chemistry of Solids*, 171, 110993. <https://doi.org/10.1016/j.jpics.2022.110993>
- [4] Jin, Q., Lu B., Pan Y., Tao X., Himmelhaver C., ... Li X., 2020, Novel porous ceramic sheet supported metal reactors for continuous-flow catalysis, *Catalysis today*, 358, 324-332. <https://doi.org/10.1016/j.cattod.2019.12.006>
- [5] Hasanpour M., Motahari S., Jing D., & Hatami M., 2021, Statistical analysis and optimization of photodegradation efficiency of methyl orange from aqueous solution using cellulose/zinc oxide hybrid aerogel by response surface methodology (RSM), *Arabian Journal of Chemistry*, 14(11), 103401. <https://doi.org/10.1016/j.arabjc.2021.103401>
- [6] Side S., Putri SE., S NI., 2023, Determination of the Effectiveness of Phenol Degradation Types Using Zeolite/TiO₂ Composites, *Proceeding of The International Conference on Science and Advanced Technology (ICSAT)*, 51: 1358–63.
- [7] Putri SE., Herawati N., Fudhail A., Pratiwi DE., Side S., ... Surleva A., 2023, Biosynthesis of copper nanoparticles using *Hylocereus costaricensis* peel extract and their photocatalytic properties, *Karbala International Journal of Modern Science*, 9(2), 289–306.
- [8] Rajappa S., Shivarathri PG., Rajappa MH., Devendrachari MC., & Kotresh HMN., 2024, Energy-efficient low-power LED-mediated effective photodegradation of cationic and anionic dyes by phthalocyanine-based COF sensitized ZnO photoactive material, *Polyhedron*, 252, 116881. <https://doi.org/10.1016/j.poly.2024.116881>
- [9] Muneeb A., Rafique MS., Murtaza MG., Arshad T., Shahadat I., Rafique M., & Nazir A., 2023, Fabrication of Ag–TiO₂ nanocomposite employing dielectric barrier discharge plasma for photodegradation of methylene blue, *Physica B: Condensed Matter*, 665, 414995. <https://doi.org/10.1016/j.physb.2023.414995>
- [10] Ramadani IWS., Ramadhani AN., & Subaer AF., 2022, The renewable of low toxicity gelcasting porous ceramic as Fe₂O₃ catalyst support on phenol photodegradation, *International Journal of Design & Nature and Ecodynamics*, 17(4), 503-511. <https://doi.org/10.18280/ijdne.170403>
- [11] Gunawan G., Prasetya NA., Widodo DS., & Wijaya RA., 2023, Electrochemical degradation of methylene blue with seawater and Pb/PbO₂ electrodes from battery waste, *Karbala International Journal of Modern Science*, 9(4), 725-741.
- [12] Boucherdoud A., Seghier A., Kherroub DE., Douinat O., Dahmani K., Bestani B., & Benderdouche N., 2025, Autogenous deposition of copper oxide onto polyaniline nanocomposite catalysts for the photodegradation of methylene blue and congo red: Experimental inquiry, RSM optimization, and DFT calculation, *Materials Science and Engineering: B*, 314, 118015. <https://doi.org/10.1016/j.mseb.2025.118015>
- [13] Kurniawan T., & Azis MA., 2024, Simultaneous impregnation-dealumination to produce SnO₂-hierarchical zeolite for methylene blue elimination via adsorption-photodegradation, *Case Studies in Chemical and Environmental Engineering*, 9, 100613. <https://doi.org/10.1016/j.cscee.2024.100613>
- [14] Ghattavi S., & Nezamzadeh-Ejhiieh A., 2020, GC-MASS detection of methyl orange degradation intermediates by AgBr/g-C₃N₄: experimental design, bandgap study, and characterization of the catalyst, *International Journal of Hydrogen Energy*, 45(46), 24636-24656. <https://doi.org/10.1016/j.ijhydene.2020.06.207>
- [15] Putri SE., Pratiwi DE., Tjahjanto RT., Desa SS., & Rahman A., 2024, The effect of starch concentration towards gelcasting porous ceramics capability as TiO₂ catalyst support in degrading methyl orange (MO) dye, In *AIP Conference Proceedings*, 2–11. <https://doi.org/10.1063/5.0182031>
- [16] Side S., Putri SE., Ilyas NM., Rahman A., Desa SS., & Subaer., 2024, The effect of sago starch concentration on the ability of Fe₂O₃-porous ceramic for phenol photodegradation, In *AIP Conference Proceedings* (Vol. 2799, No. 1, p. 020140). AIP Publishing LLC. <https://doi.org/10.1063/5.0182036>
- [17] Liao M., Guo C., Guo W., Hu T., Qin H., Gao P., & Xiao H., 2020, Hydrogen production in microreactor using porous SiC ceramic with a pore-in-pore hierarchical structure as catalyst



- support, *International Journal of Hydrogen Energy*, 45(41), 20922-20932. <https://doi.org/10.1016/j.ijhydene.2020.05.244>
- [18] Fedotov AS., Uvarov VI., Tsodikov MV., Paul S., Simon P., Marinova M., & Dumeignil F., 2021, Production of styrene by dehydrogenation of ethylbenzene on a [Re, W]/ γ -Al₂O₃ (K, Ce)/ α -Al₂O₃ porous ceramic catalytic converter, *Chemical Engineering and Processing-Process Intensification*, 160, 108265. <https://doi.org/10.1016/j.cep.2020.108265>
- [19] Woranuch W., Ngaosuwan K., Kiatkittipong W., Wongsawaeng D., Appamana W., ... Assabumrungra S., 2022, Fine-tuned fabrication parameters of CaO catalyst pellets for transesterification of palm oil to biodiesel, *Fuel*, 323, 124356. <https://doi.org/10.1016/j.fuel.2022.124356>
- [20] Putri SE., Pratiwi DE., Tjahjanto RT., Ilyas NM., Tahir D., Rahman A., & Heryanto H., 2023, Effect of Sintering Temperature on the Microstructure Behavior of Gelcasted Porous Ceramics Using Cassava Starch as Pore Template, *Indonesian Journal of Chemistry*, 23(5), 1199-1211.
- [21] da Cruz Lima E., Nobre FX., da Silva Ferreira N., Moraes CAF., Rocha JM., ... de Matos JME., 2025, Optimization of photocatalytic parameters for the photodegradation of hydroxychloroquine sulfate using the Ag/Cu-TNT nanocomposite, *Journal of Water Process Engineering*, 71, 107205. <https://doi.org/10.1016/j.jwpe.2025.107205>
- [22] Rhithuparna D., Ghosh N., Khatoun R., Rokhum SL., & Halder G., 2024, Evaluating the commercial potential of Cocos nucifera derived biochar catalyst in biodiesel synthesis from Kanuga oil: Optimization, kinetics, thermodynamics, and process cost analysis, *Process Safety and Environmental Protection*, 183, 859-874. <https://doi.org/10.1016/j.psep.2024.01.030>
- [23] Abisha P., Jinita CG., & Sonia S., 2025, Porous Metal Organic Framework (MOF) derived dimorphic (n-ZnO/p-NiO) Z-scheme heterojunction anchored with MWCNTs (ternary nano-architecture): A novel approach for optimization of photodegradation mechanism and kinetics of Congo red (CR) dye, *Physica E: Low-dimensional Systems and Nanostructures*, 165, 116076. <https://doi.org/10.1016/j.physe.2024.116076>
- [24] Simbi I., Aigbe UO., Oyekola O., & Osibote OA., 2022, Optimization of biodiesel produced from waste sunflower cooking oil over bi-functional catalyst, *Results in Engineering*, 13, 100374. <https://doi.org/10.1016/j.rineng.2022.100374>
- [25] Ghanbari M., Abdi A., Abedi P., Mehrizadeh H., Ziarani GM., Badieli A., & Irvani S., 2024, Optimization and experimental design of photodegradation of Acid Blue-92 dye with magnetic ternary nanocomposite based on carbon nitride under visible light irradiation, *Inorganic Chemistry Communications*, 170, 113147. <https://doi.org/10.1016/j.inoche.2024.113147>
- [26] Souza IP., Crespo LH., Spessato L., Melo SA., Martins AF., Cazetta AL., & Almeida VC., 2021, Optimization of thermal conditions of sol-gel method for synthesis of TiO₂ using RSM and its influence on photodegradation of tartrazine yellow dye, *Journal of Environmental Chemical Engineering*, 9(2), 104753. <https://doi.org/10.1016/j.jece.2020.104753>

